

「ストレンジネスを含むクォーク多体系分野の理論的将来を考える」
研究会、平成21年2月27日、熱海

Kaon核生成スペクトル： ポールは見えるか？

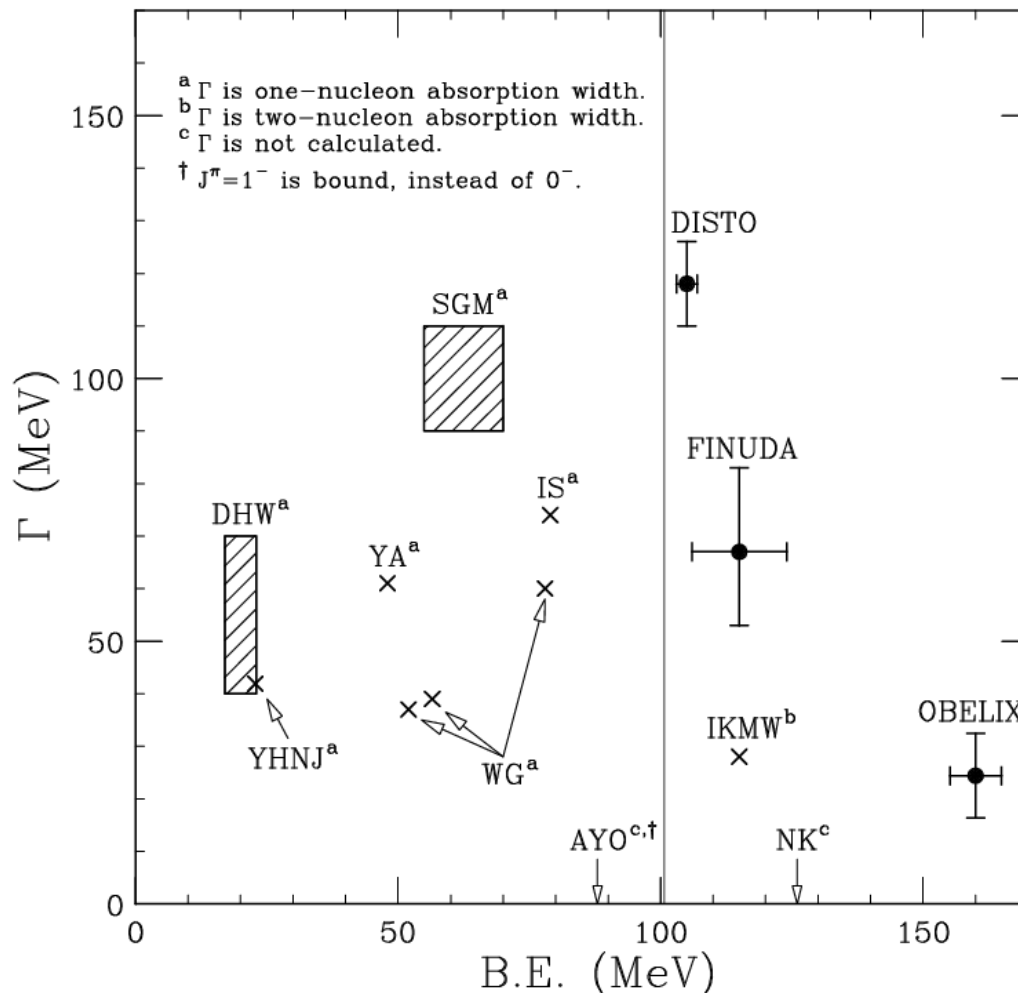
小池 貴久

理研 仁科センター

原田 融

大阪電気通信大学

“K⁻pp” is suggested to be the lightest and most fundamental kaonic nuclei, but the theoretically-calculated and experimentally-measured *B.E.* and Γ are not converged!



Theory

- **YA:** Yamazaki, Akaishi
- **SGM:** Shevchenko, Gal, Mares
- **IS:** Ikeda, Sato
- **DHW:** Dote, Hyodo, Weise
- **IKMW:** Ivanov, Kleine *et al.*
- **NK:** Nishikawa & Kondo
- **AYO:** Arai, Yasui, Oka
- **YHNJ:** Yamagata, Hirenzaki *et al.*
- **WG:** Wychech, Green,

Experiment

- **FINUDA**
- **OBELIX**
- **DISTO**

◆ New measurement for searching “K⁻pp”

★ M. Iwasaki, T. Nagae *et al.*, **J-PARC E15 experiment**

³He(In-flight K⁻, n) “K⁻pp”
at $p_{K^-} = 1 \text{ GeV}/c$ and $\theta_n = 0^\circ$

+

“K⁻pp” $\rightarrow \Lambda p \rightarrow \pi^- pp$
detecting all charged particles
from the decay of “K⁻pp”

missing-mass
spectroscopy

Simultaneous measurement

invariant-mass
spectroscopy

Our purpose:

Theoretical calculation of **³He(In-flight K⁻, n) inclusive/semi-exclusive spectra** within the DWIA framework using Green’s function method.

Refs. T. Koike & T. Harada, Phys. Lett. B652 (2007) 262-268.

T. Koike & T. Harada, Nucl. Phys. A804 (2008) 231-273.

◆ **Theoretical calculations of $^3\text{He}(\text{In-flight } K^-, n)$ reaction spectrum for J-PARC E15 experiment**

- **Case using Yamazaki-Akaishi's optical potential:**

$B.E. \sim 50 \text{ MeV}, \Gamma \sim 60 \text{ MeV}$

→ The clear K^-pp formation peak would be observed!

T. Koike & T. Harada, Phys. Lett. B652 (2007) 262-268.

- **Case using the potential based on chiral unitary model:
less binding than YA case ($B.E. \sim 20 \text{ MeV}$)**

→ We can still recognize a peak structure.

J. Yamagata *et al.*, Mod. Phys. Lett. A23 (2008) 2528-2531; arXiv:0812.4359

- **Case simulating Faddeev calculations:**

more binding than YA case ($B.E. \sim 70\text{-}80 \text{ MeV}$)

→ The cusp-like peak appears at $K^{\text{bar}}N \rightarrow \Sigma \pi$ decay threshold.

T. Koike & T. Harada, Mod. Phys. Lett. A23 (2008) 2540-2543.

◆ Distorted-Wave Impulse Approximation (DWIA)

$$\frac{d^2\sigma}{dE_n d\Omega_n} = \beta \left[\frac{d\sigma}{d\Omega_n} \right]^{(\text{elem})} S(E)$$

Kinematical factor \nearrow \uparrow \curvearrowright **Strength function**
Fermi-averaged elementary cross-section
 $K^- + n \rightarrow n + K^-$ in lab. system

Morimatsu & Yazaki's Green function method Prog.Part.Nucl.Phys.33(1994)679.

$$S(E) = -\frac{1}{\pi} \text{Im} \left[\sum_{\alpha, \alpha'} \int d\mathbf{r} d\mathbf{r}' f_{\alpha}(\mathbf{r}) G_{\alpha, \alpha'}(E; \mathbf{r}, \mathbf{r}') f_{\alpha'}(\mathbf{r}') \right]$$

Green's function K^-pp system \rightarrow employing K^- – "pp" optical potential

$$G_{\alpha, \alpha'}(E; \mathbf{r}, \mathbf{r}') = \langle \alpha | \psi_{K^-}(\mathbf{r}) \frac{1}{E - H_{K^-pp}^{\text{opt.}} + i\epsilon} \psi_{K^-}^{\dagger}(\mathbf{r}') | \alpha' \rangle$$

recoil effect

$$f_{\alpha}(\mathbf{r}) = \chi^{(-)*} \left(\mathbf{p}_n, \frac{M_{pp}}{M_{3\text{He}}} \mathbf{r} \right) \chi^{(+)} \left(\mathbf{p}_{K^-}, \frac{M_{pp}}{M_{3\text{He}}} \mathbf{r} \right) \langle \alpha | \psi_n(\mathbf{r}) | i \rangle$$

Distorted wave for incoming(+)/outgoing(-) particles
 \rightarrow Eikonal approximation

neutron hole wave function
 \rightarrow (0s)³ harmonic oscillator model

◆ Distorted-Wave Impulse Approximation (DWIA)

$$\frac{d^2\sigma}{dE_n d\Omega_n} = \beta \left[\frac{d\sigma}{d\Omega_n} \right]^{(\text{elem})} S(E)$$

Kinematical factor β $\left[\frac{d\sigma}{d\Omega_n} \right]^{(\text{elem})}$ Strength function $S(E)$
 Fermi-averaged elementary cross-section
 $K^- + n \rightarrow n + K^-$ in lab. system

Some notes on (K^- , N) reaction:

- Kinematical factor $\beta \sim 2$ for *backward* $K^- + N$ scattering.
- The *Fermi-averaged* elementary cross-section is reduced by $\sim 60\%$, compared to *free-space* value.
- The contribution from $K^- + p \rightarrow n + K^{\text{bar}0}$ enhances the cross section by $\sim 18\%$.

c.f. J. Yamagata-Sekihara *et al.*, arXiv:0812.4359

For details, see

T. Koike and T. Harada, Nucl. Phys. A804 (2008) 231-273.

◆ Energy-dependent K^- -“pp” optical potential

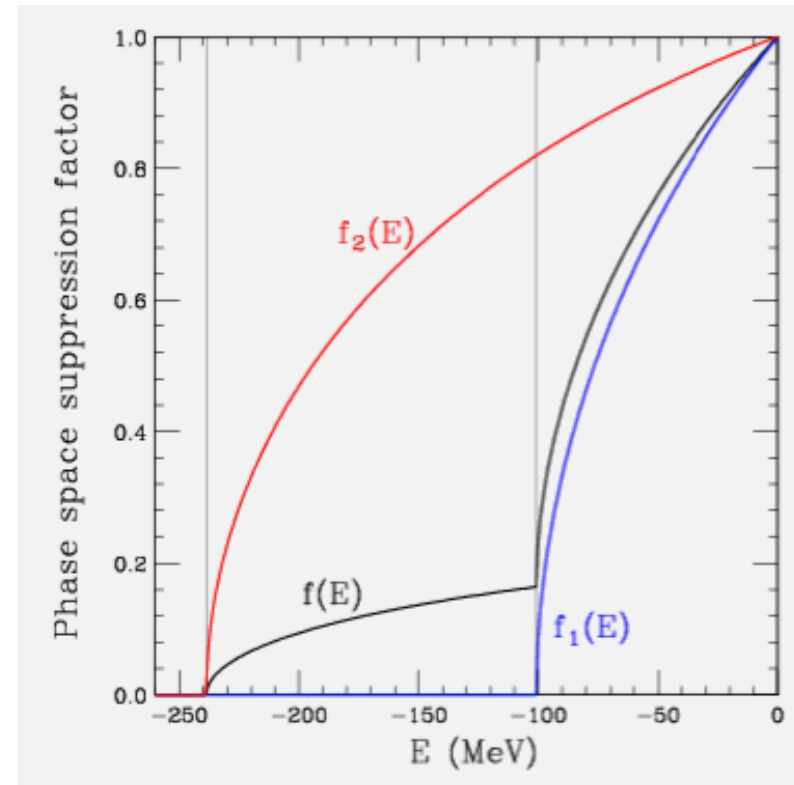
$$U_{K^-pp}^{\text{opt.}}(r) = (V_0 + i W_0 \underbrace{f(E)}_{\substack{\uparrow \\ \text{phase space factor}}}) \exp [-(r/b)^2]$$

$$f(E) = 0.8 f_1(E) + 0.2 f_2(E)$$

- $f_1(E)$: 1-nucleon K^- abs.



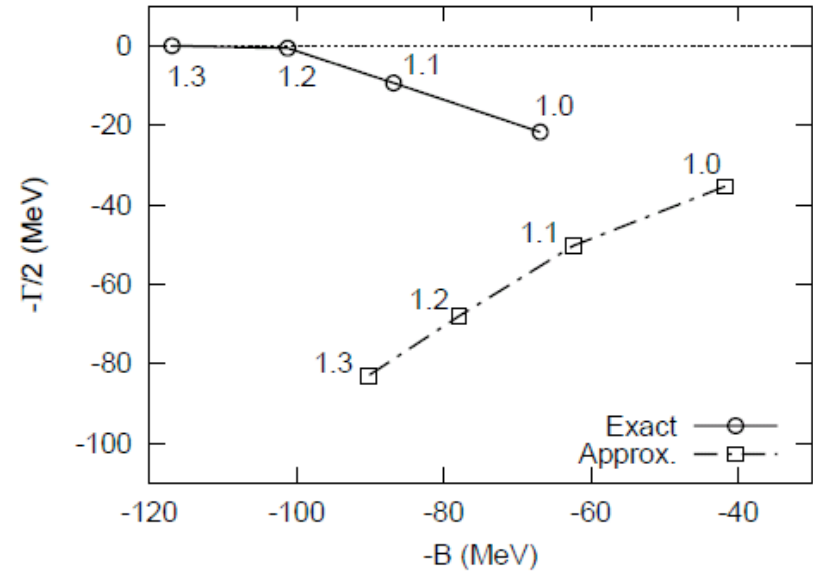
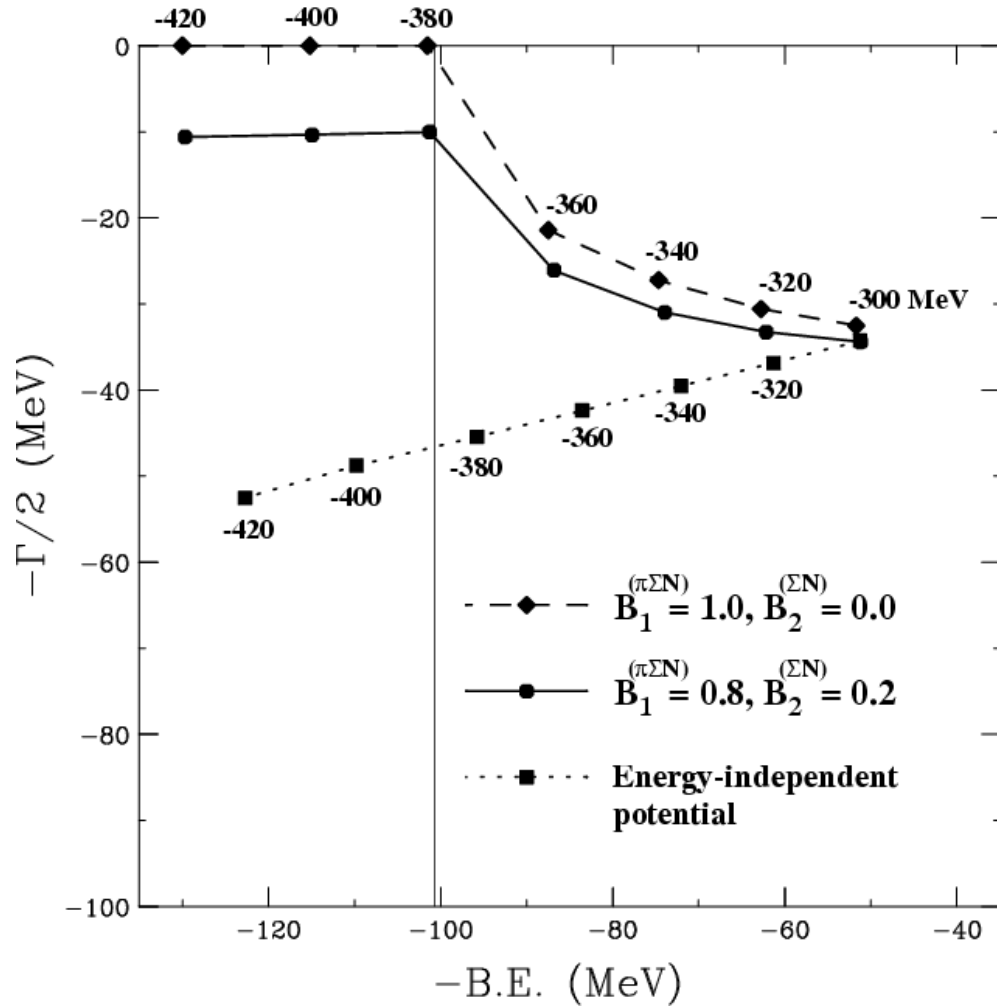
- $f_2(E)$: 2-nucleon K^- abs.



Ref. J. Mares, E. Friedman, A. Gal, PLB606 (2005) 295.

J. Yamagata, H. Nagahiro, S. Hirenzaki, PRC74 (2006) 014604.

V_0 is changed with fixing $W_0 = -93$ MeV
in our optical potential model.



Ikeda&Sato, Faddeev calculation
arXiv:0809.1285

◆ Single-channel Green's function

$$\{(E - V_{\text{Coul}}(\mathbf{r}))^2 + \nabla^2 - \mu^2 - 2\mu \underline{U^{\text{opt}}(E; \mathbf{r})}\} G(E; \mathbf{r}, \mathbf{r}') = \delta^3(\mathbf{r} - \mathbf{r}'),$$

▪ K⁻-”pp” optical potential

$$U^{\text{opt}}(E; \mathbf{r}) = (V_0 + i W_0 f(E)) \exp[-(\mathbf{r}/b)^2]$$

↑ phase space factor

The Klein-Gordon equation is solved self-consistently in complex E -plane;

$$\{(\omega(E) - V_{\text{Coul}}(\mathbf{r}))^2 + \nabla^2 - \mu^2 - 2\mu \underline{U^{\text{opt}}(E; \mathbf{r})}\} \Phi(E; \mathbf{r}) = 0,$$

$$\longrightarrow \begin{cases} \text{Re } \omega(E) = -B.E. = E, \\ \text{Im } \omega(E) = -\Gamma/2 \end{cases}$$

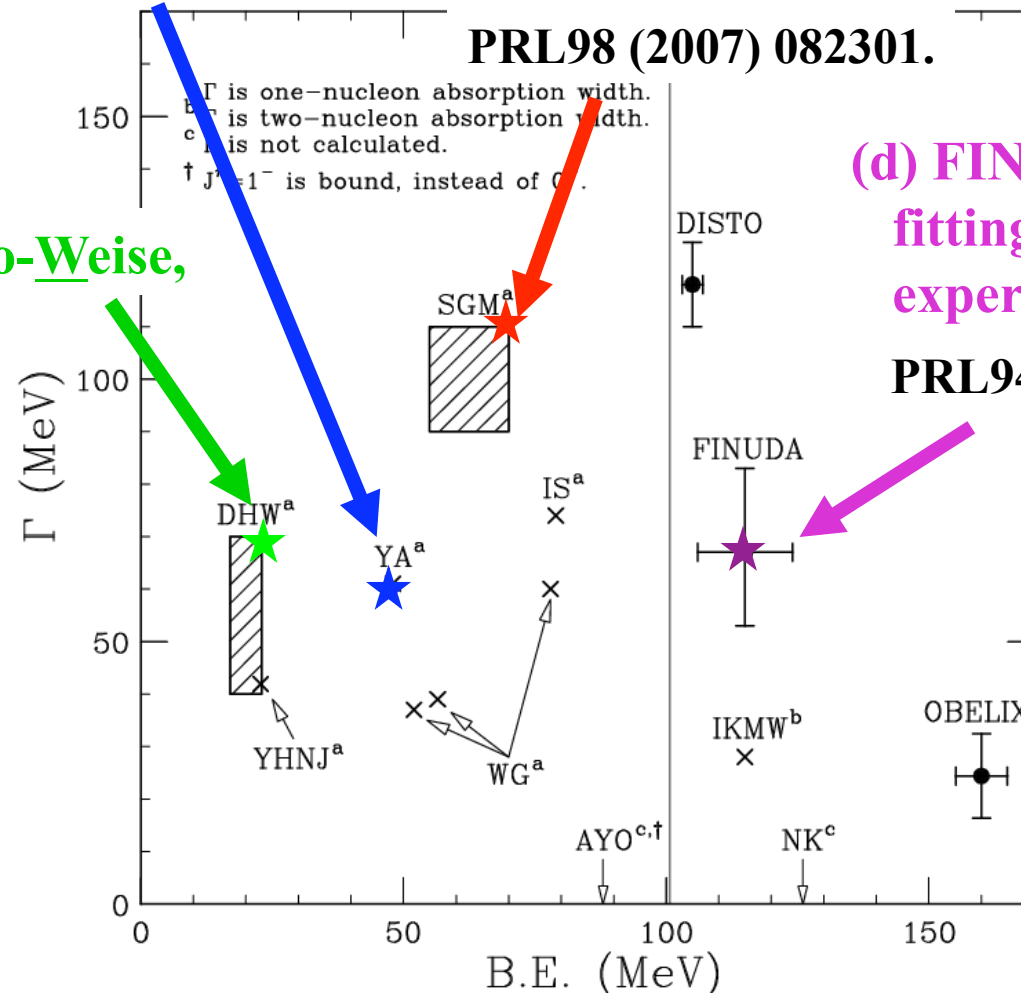
We simulate the following 4 kinds of the calculations/experiment;

**(b) YA: Yamazaki-Akaishi,
variational cal.
with phenomenological $K^{\text{bar}}N$ int.
PLB535 (2002) 70.**

**(a) SGM: Shevchenko-Gal-Mares,
Faddeev cal.
with phenomenological $K^{\text{bar}}N$ int.
PRL98 (2007) 082301.**

**(c) DHW: Dote-Hyodo-Weise,
variational cal.
with Chiral SU(3)
based $K^{\text{bar}}N$ int.
NPA804 (2008) 197.**

**(d) FINUDA:
fitting to FINUDA
experimental data
PRL94 (2005) 212303.**



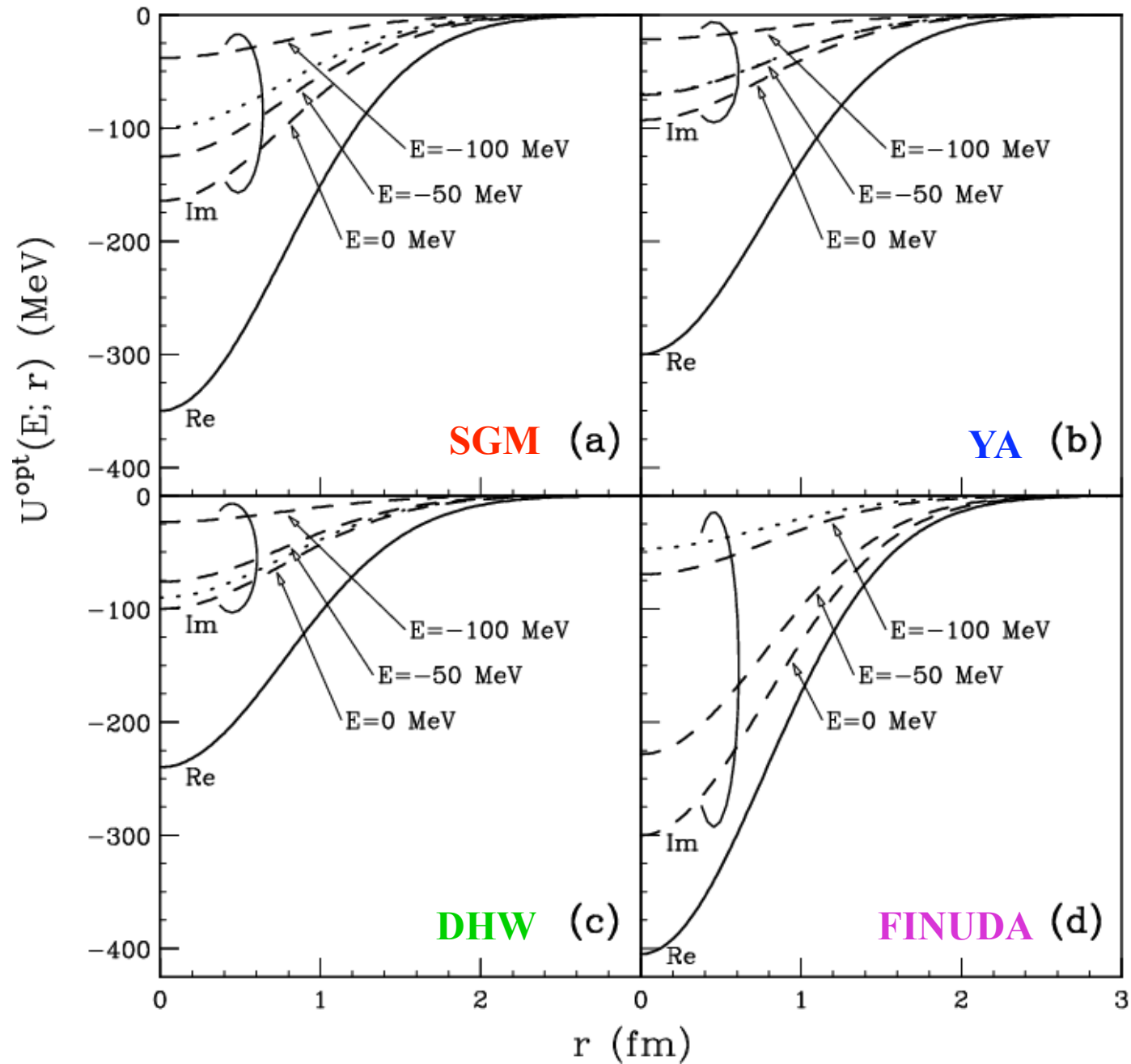
◆ Parameters of the employed optical potentials

	Potentials	V_0 (MeV)	W_0 (MeV)	B.E. (MeV)	Γ (MeV)
(a)	SGM	-350	-165	72	115
(b)	YA	-300	-93	51	68
(c)	DHW	-240	-100	22	69
(d)	FINUDA	-405	-300	116	67

* $b = 1.09$ fm for all potentials;

The shrinking effect of the core nucleus is small.

◆ Employed K^- -”pp” optical potentials



◆ **Decomposition of strength function into K^- escape / K^- conversion part**

$$\text{Im } G = (1 + G^\dagger U^\dagger)(\text{Im } G_0)(1 + UG) + G^\dagger(\text{Im } U)G,$$

where $G = G_0 + G_0 U G$, G_0 ; Free Green's function

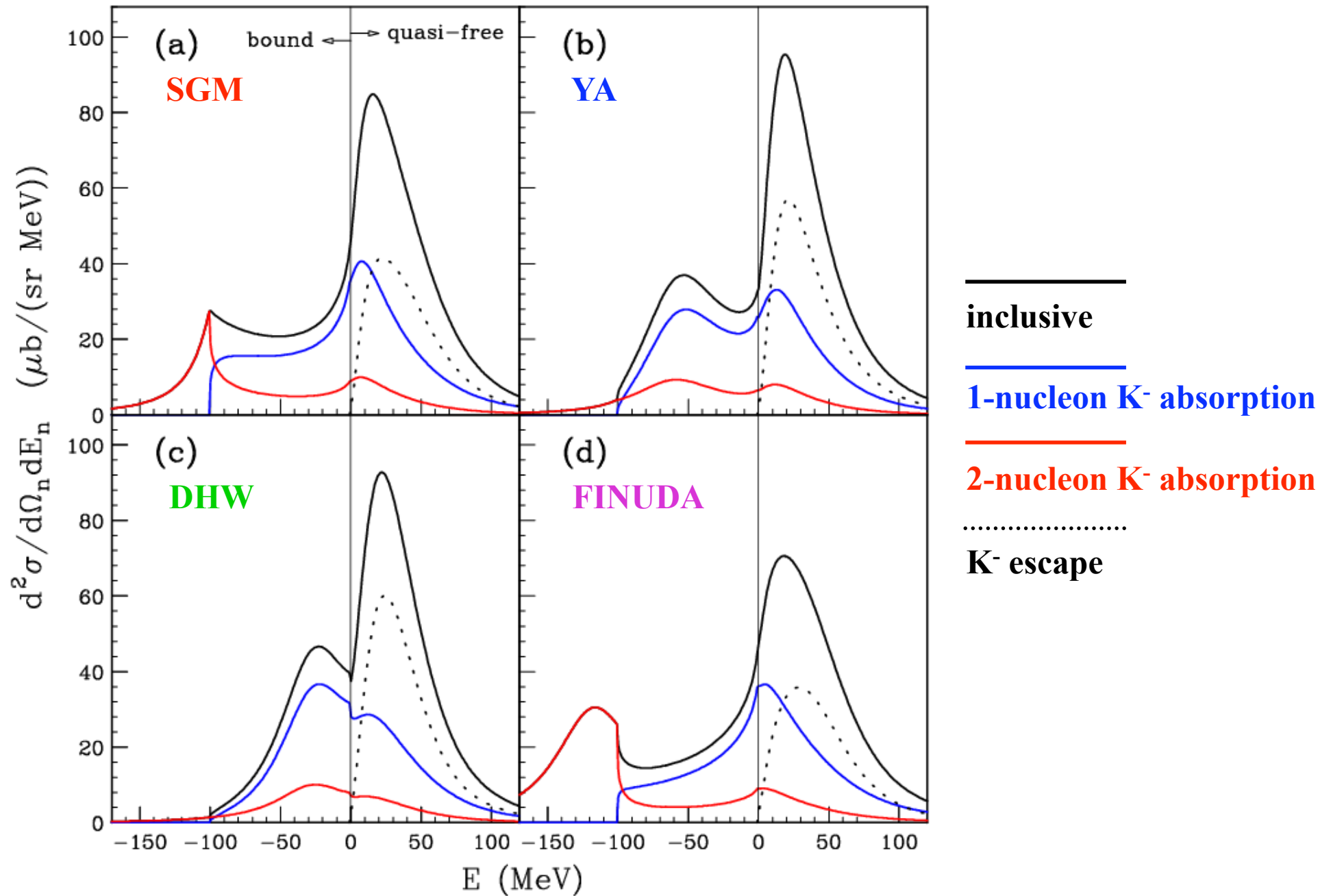
$$S = S^{\text{esc}} + S^{\text{con}}$$

$$\begin{cases} S^{\text{esc}} = -\frac{1}{\pi} F^\dagger (1 + G^\dagger U^\dagger)(\text{Im } G_0)(1 + UG)F ; \mathbf{K^- \text{ escape}} \\ S^{\text{con}} = -\frac{1}{\pi} F^\dagger G^\dagger (\text{Im } \underline{U}) G F ; \mathbf{K^- \text{ conversion}} \end{cases}$$

↑ optical potential

★ K^- conversion spectrum is actually measured in J-PARC experiment.

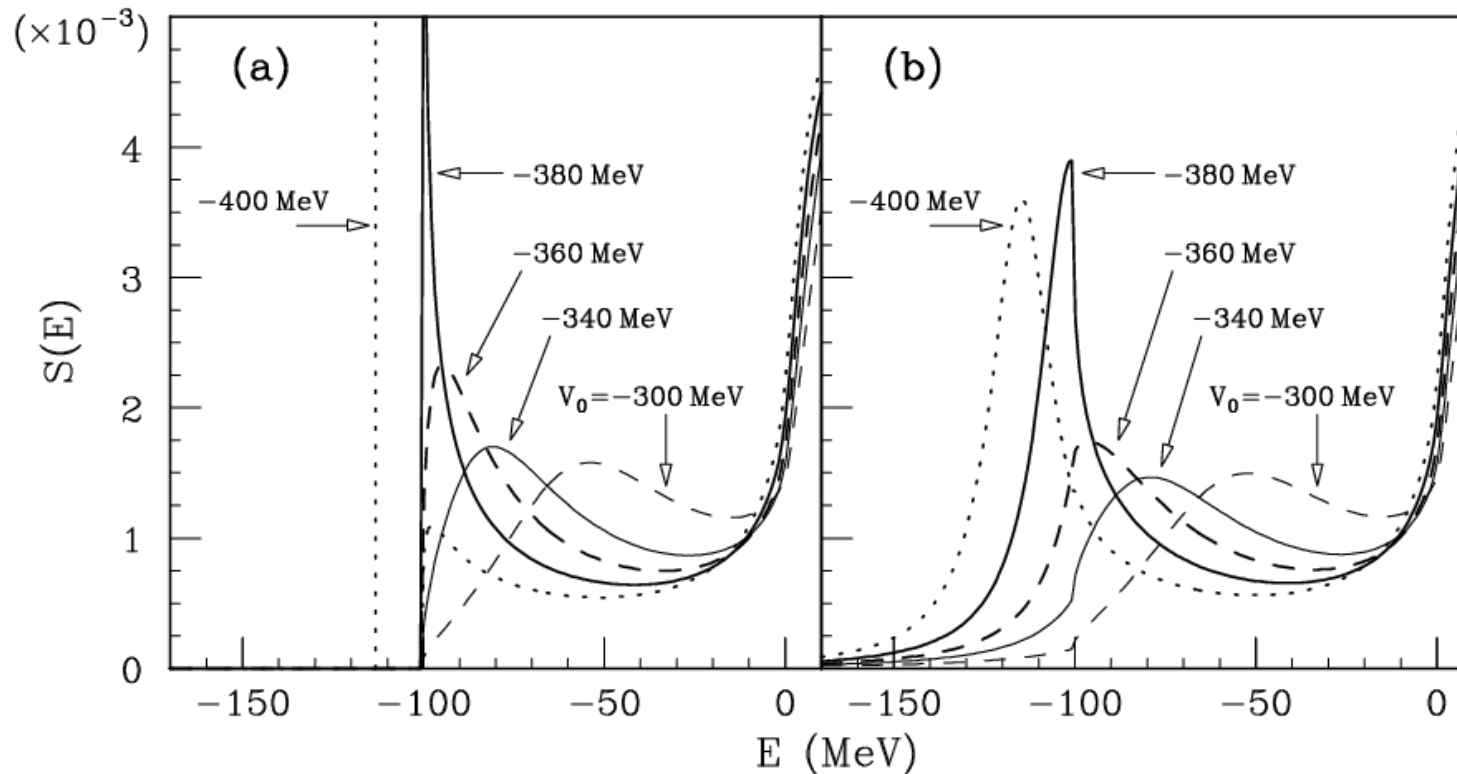
◆ Decomposition into semi-exclusive spectra



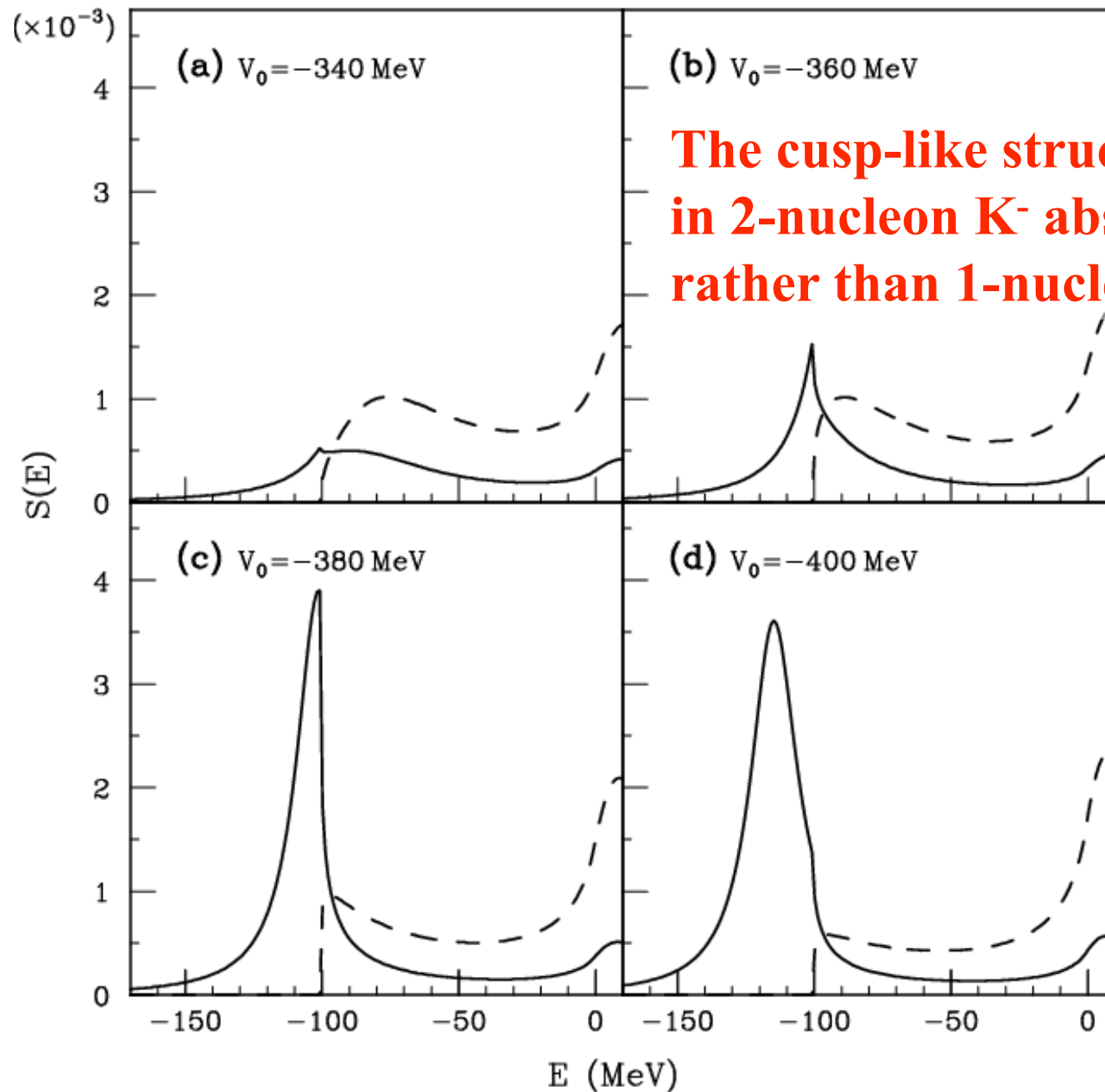
◆ Dependence on the real part strength V_0

(a) $\begin{cases} B_1^{(\pi\Sigma N)} = 1.0 \\ B_2^{(\Sigma N)} = 0.0 \end{cases}$

(b) $\begin{cases} B_1^{(\pi\Sigma N)} = 0.8 \\ B_2^{(\Sigma N)} = 0.2 \end{cases}$



* W_0 is fixed to be -93 MeV.



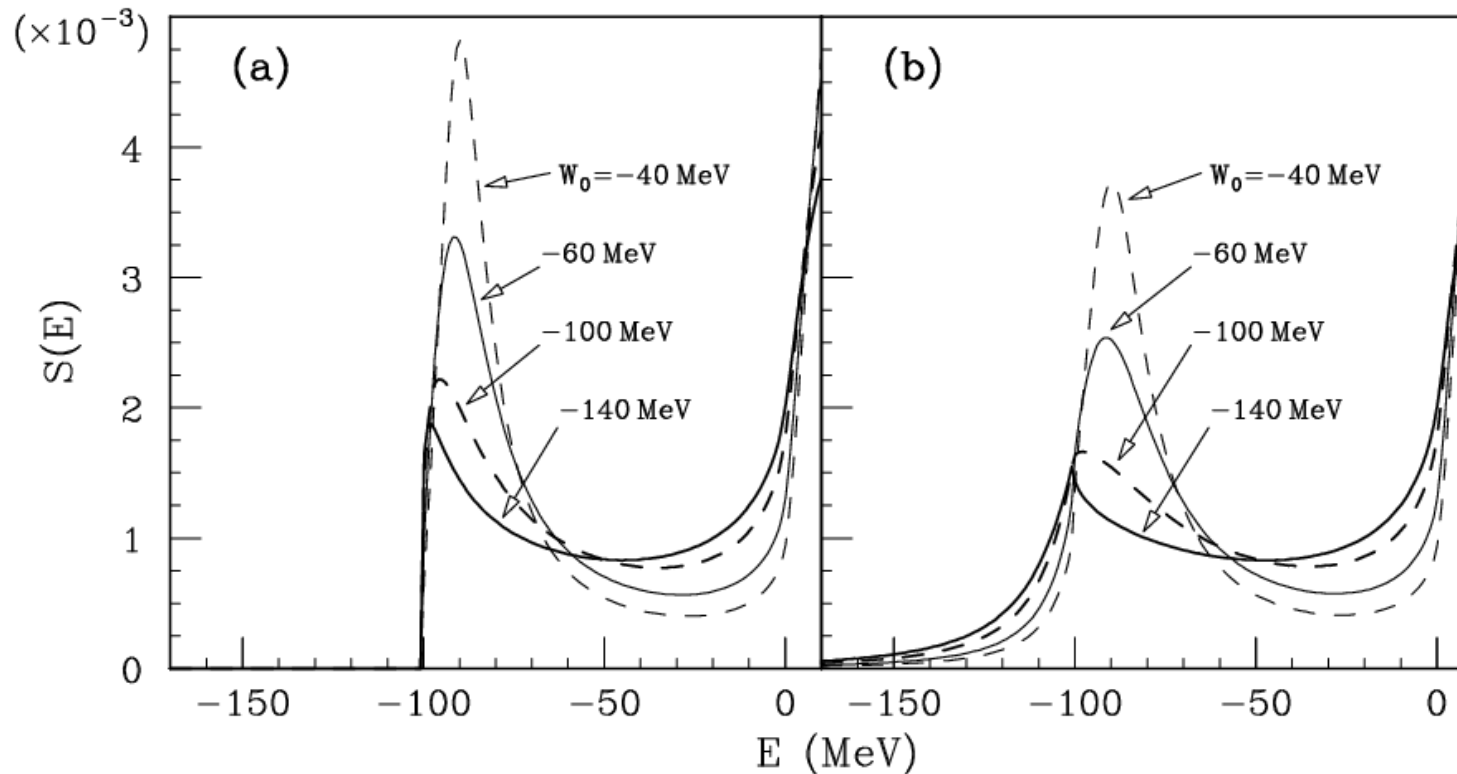
The cusp-like structure would appear in 2-nucleon K^- absorption spectrum, rather than 1-nucleon one.

1-nucleon K^- absorption

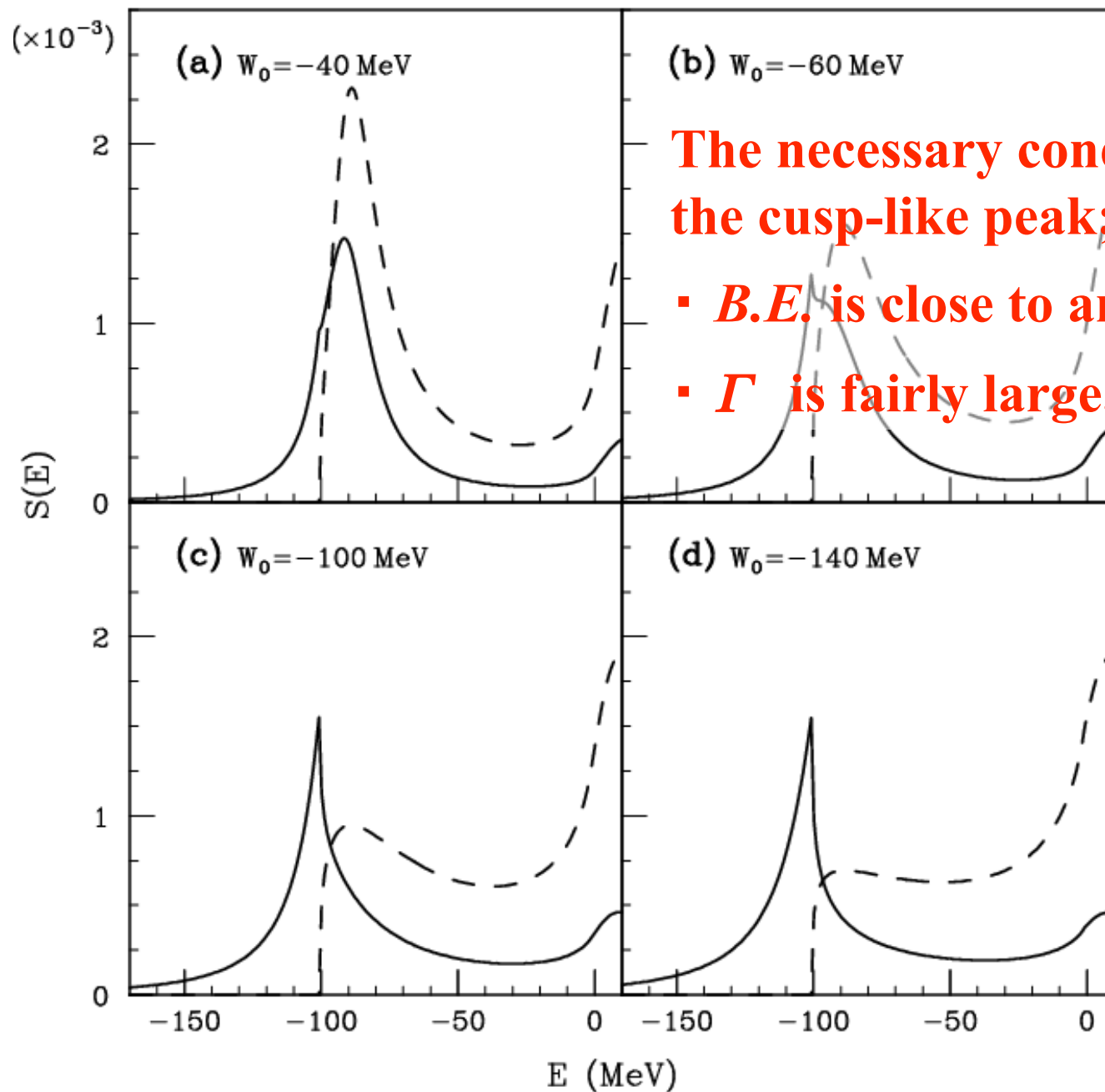
—————
2-nucleon K^- absorption

◆ Dependence on the imaginary part strength W_0

$$(a) \begin{cases} B_1^{(\pi\Sigma N)} = 1.0 \\ B_2^{(\Sigma N)} = 0.0 \end{cases} \quad (b) \begin{cases} B_1^{(\pi\Sigma N)} = 0.8 \\ B_2^{(\Sigma N)} = 0.2 \end{cases}$$



* V_0 is fixed to be -360 MeV.



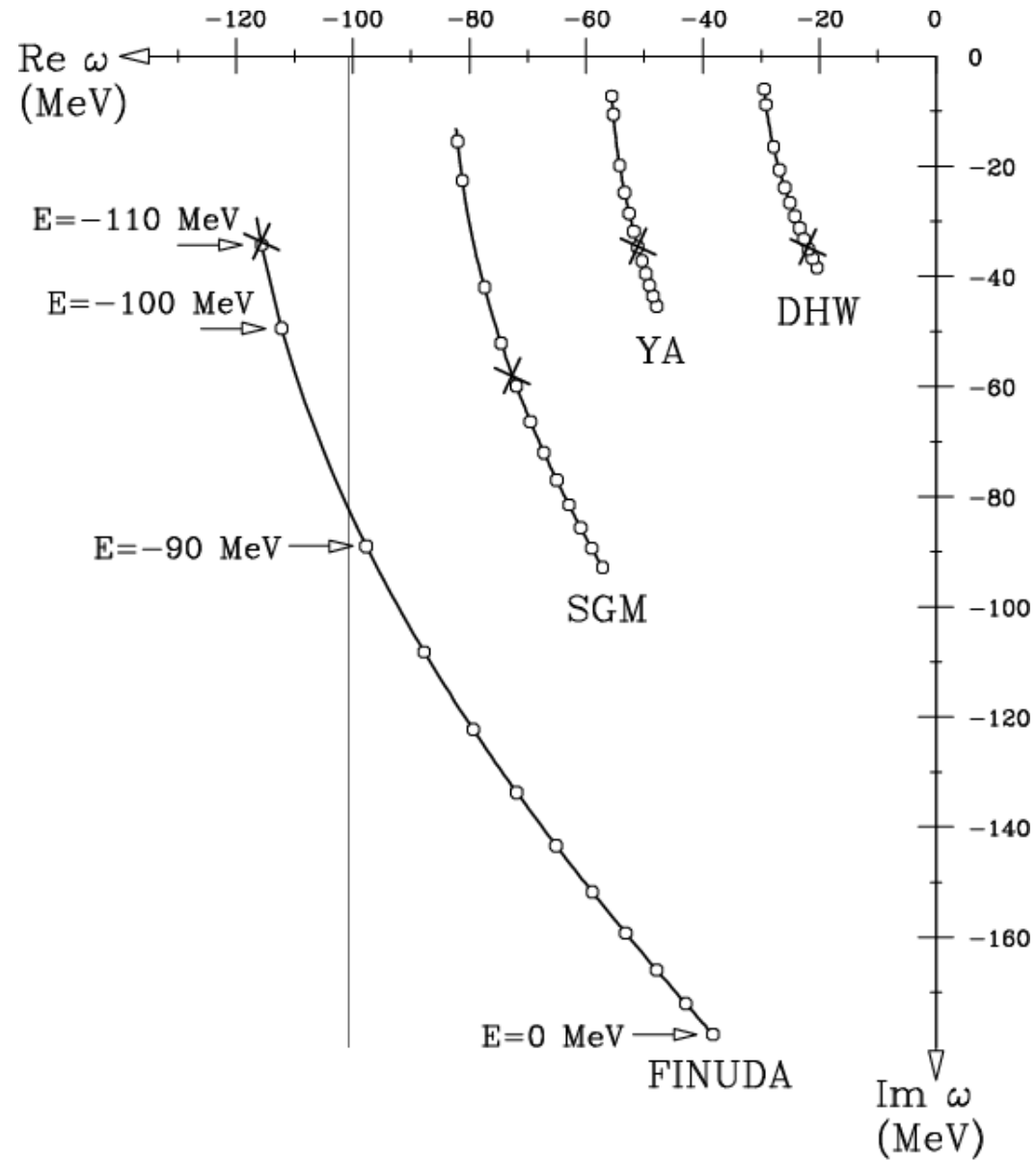
The necessary conditions to appear the cusp-like peak;

- $B.E.$ is close to and above $E_{th}(\pi\Sigma N)$.
- Γ is fairly large.

1-nucleon K^- absorption

—————
2-nucleon K^- absorption

◆ Pole trajectory in complex E -plane



$$S^{(\text{pole})}(E) \simeq -\frac{1}{\pi} \frac{\text{Im } \omega(E)}{(E - \text{Re } \omega(E))^2 + (\text{Im } \omega(E))^2}$$

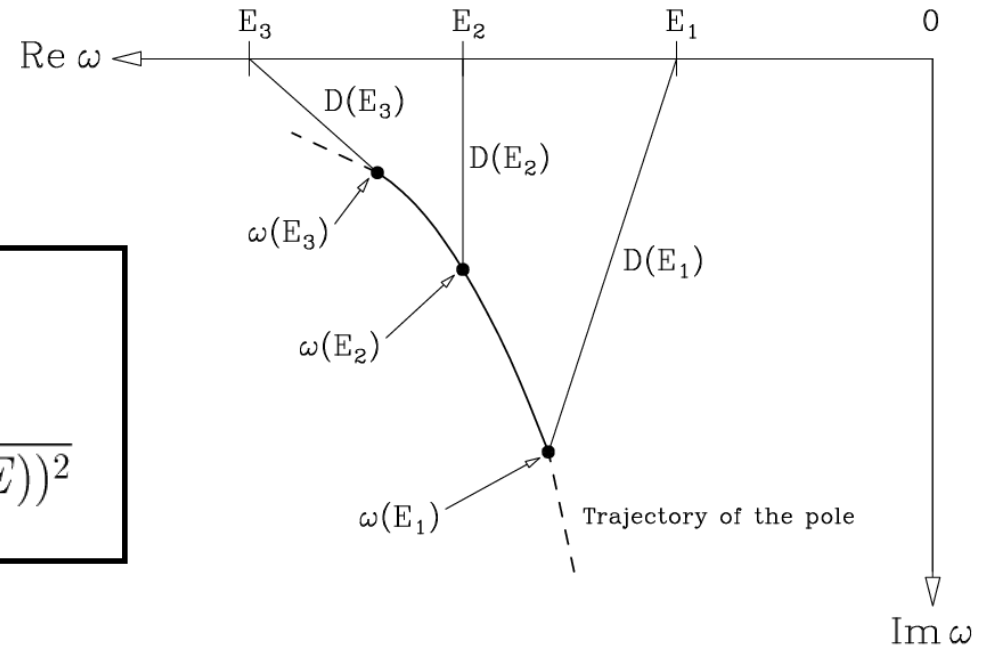
$$\text{Im } \omega(E) \propto f(E)$$

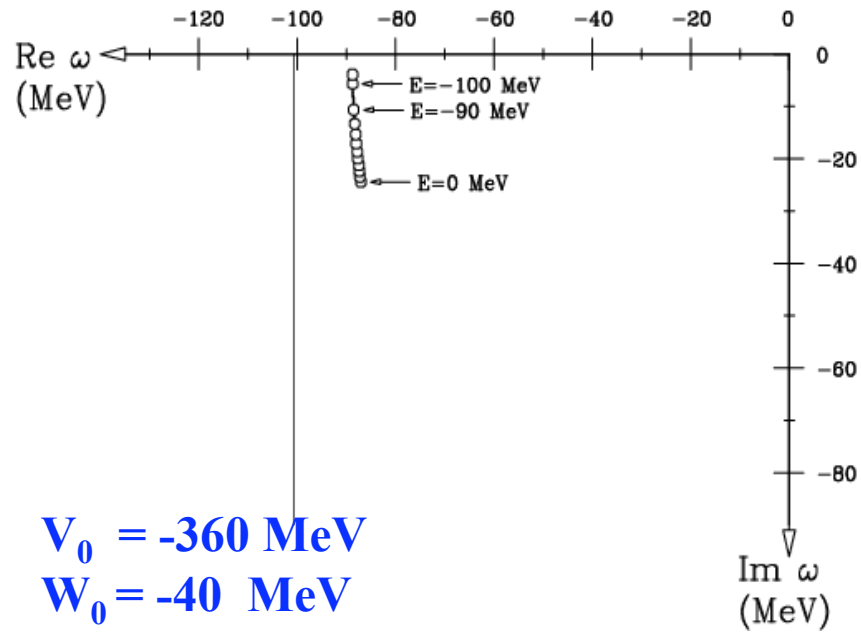
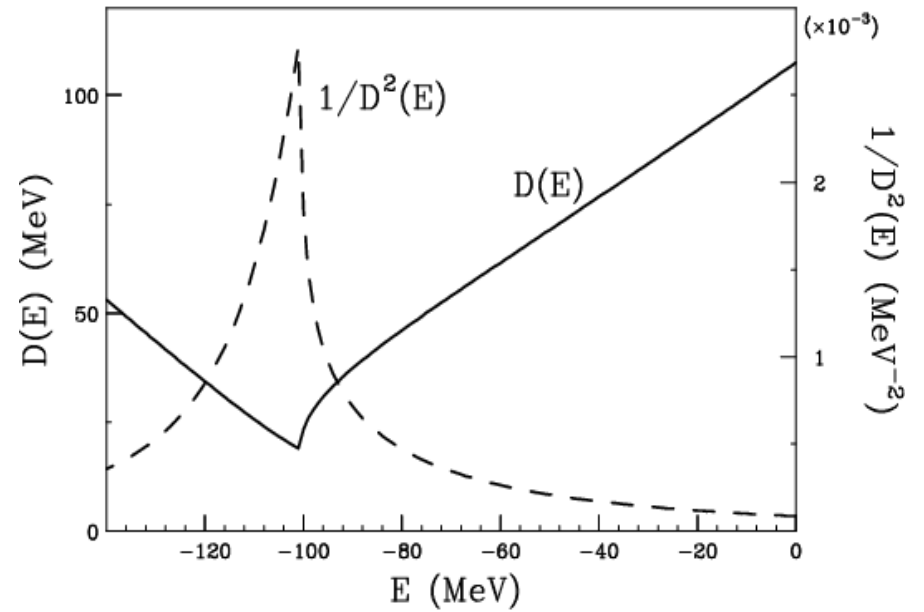
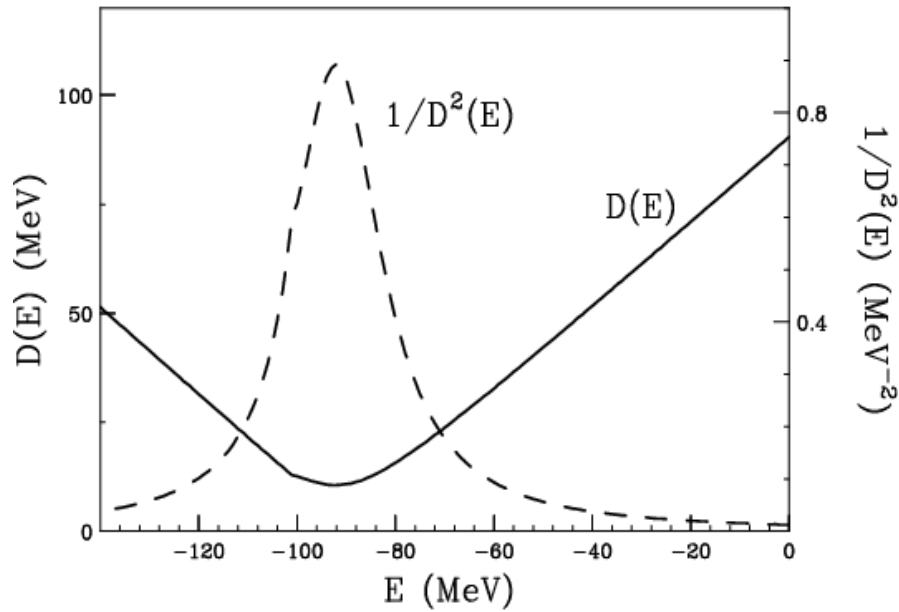
$$S^{\text{con}}(E) \approx \text{const.} \times \frac{f(E)}{D^2(E)}$$

$$D(E) \equiv \sqrt{(E - \text{Re } \omega(E))^2 + (\text{Im } \omega(E))^2}$$

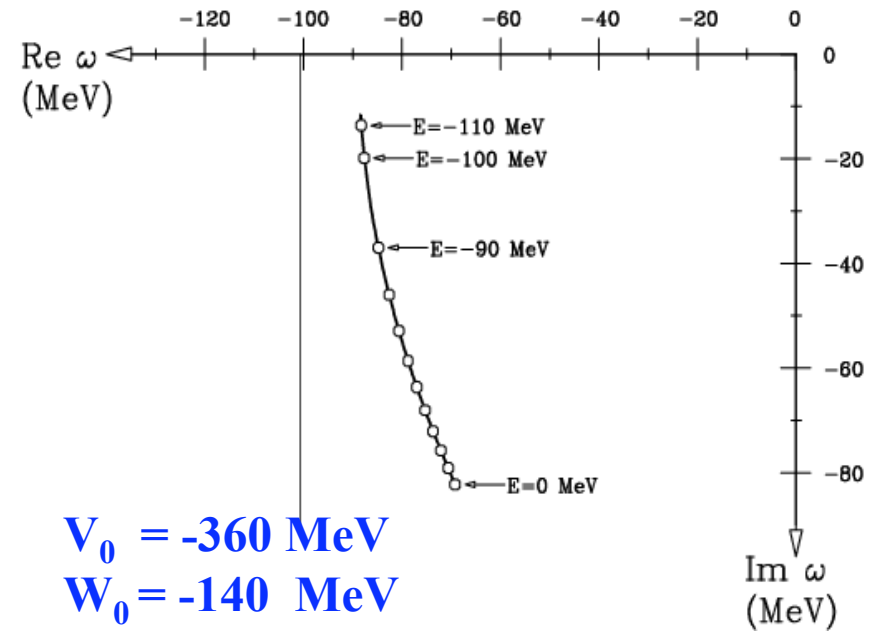
$$S_1^{\text{con}}(E) \approx \text{const.} \times \frac{f_1(E)}{D^2(E)}$$

$$S_2^{\text{con}}(E) \approx \text{const.} \times \frac{f_2(E)}{D^2(E)} \approx \text{const.} \times \frac{1}{D^2(E)}$$



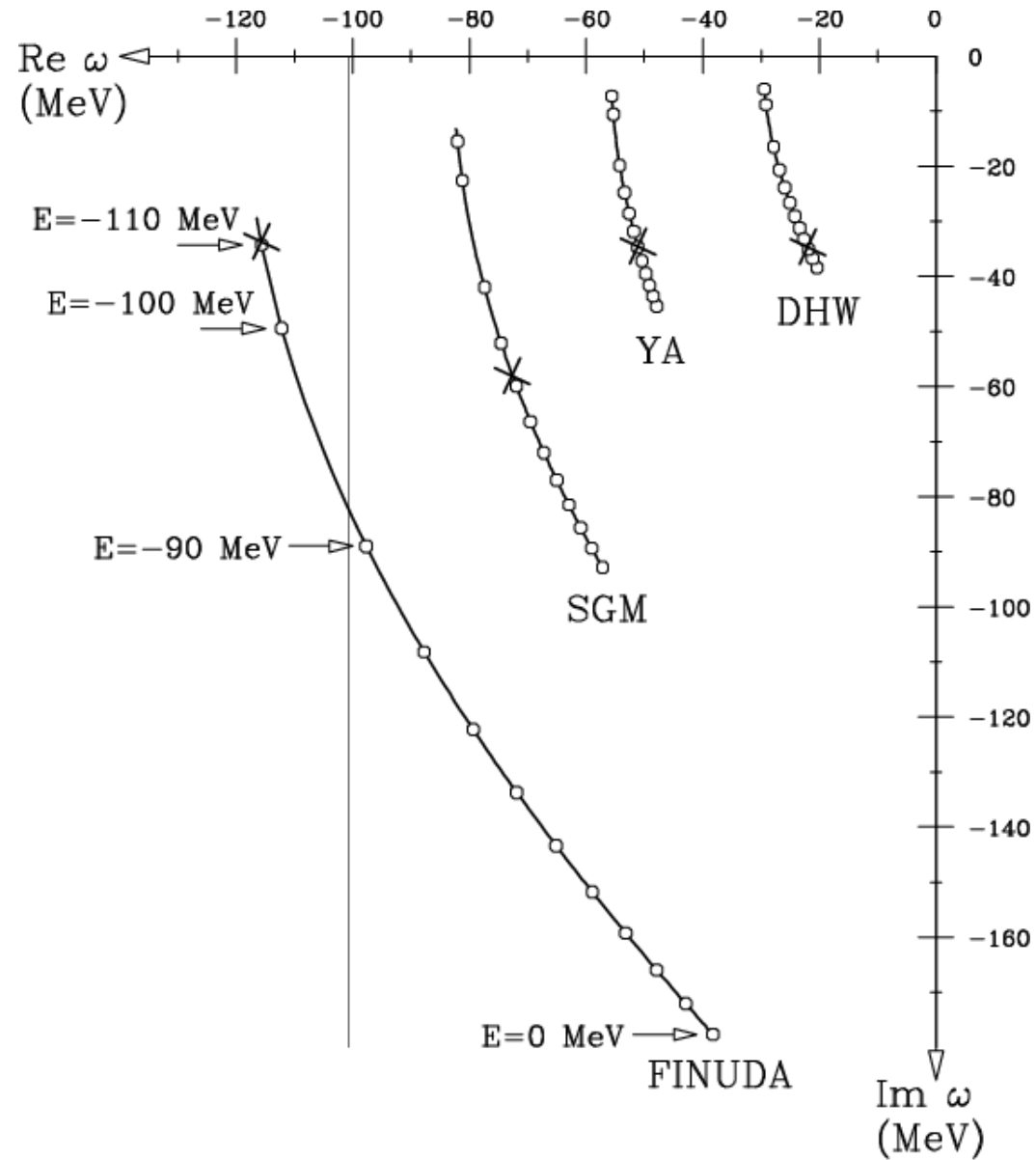


$V_0 = -360$ MeV
 $W_0 = -40$ MeV



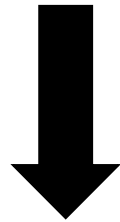
$V_0 = -360$ MeV
 $W_0 = -140$ MeV

◆ Pole trajectory in complex E -plane



For the better description of the $\Sigma\pi N$ decay threshold effect (e.g. cusp-like structure), we extend

$K^- pp$ single-channel DWIA



$(K^- p)p - (\Sigma \pi)N$ coupled-channel DWIA

◆ K⁻pp Single-channel Green's function

$$\{(E - V_{\text{Coul}}(\mathbf{r}))^2 + \nabla^2 - \mu^2 - 2\mu \underline{U^{\text{opt}}(E; \mathbf{r})}\} G(E; \mathbf{r}, \mathbf{r}') = \delta^3(\mathbf{r} - \mathbf{r}'),$$

- K⁻“pp” optical potential

$$U^{\text{opt}}(E; \mathbf{r}) = (V_0 + i W_0 f(E)) \exp[-(\mathbf{r}/b)^2]$$

↑ phase space factor

◆ (K-p)p – (πΣ)N Coupled-channel Green's function

$$\begin{bmatrix} E_1 - T_2^\ell - U_1(r) & -U_{1,2}(r) \\ -U_{2,1}(r) & E_2 - T_2^\ell - U_2(r) \end{bmatrix} \begin{bmatrix} G_{1,1}^{(\ell)}(r, r') & G_{1,2}^{(\ell)}(r, r') \\ G_{2,1}^{(\ell)}(r, r') & G_{2,2}^{(\ell)}(r, r') \end{bmatrix}$$

$$\begin{cases} T_i^\ell = \frac{\hbar^2}{2\mu_i} \left\{ -\frac{\partial^2}{\partial r^2} + \frac{\ell(\ell+1)}{r^2} \right\}, & i = 1, 2, \\ E_2 = E_1 - E_{\text{th}}(\pi\Sigma N). \end{cases} = \begin{bmatrix} \delta(r' - r) & 0 \\ 0 & \delta(r' - r) \end{bmatrix}$$

Preliminary

- **Channel 1 = K-p, channel 2 = πΣN**
- Ch.1 において “pp” core を固めているのと同様に、Ch.2 でも “ΣN” core を固める。→ 境界条件は正しくない。

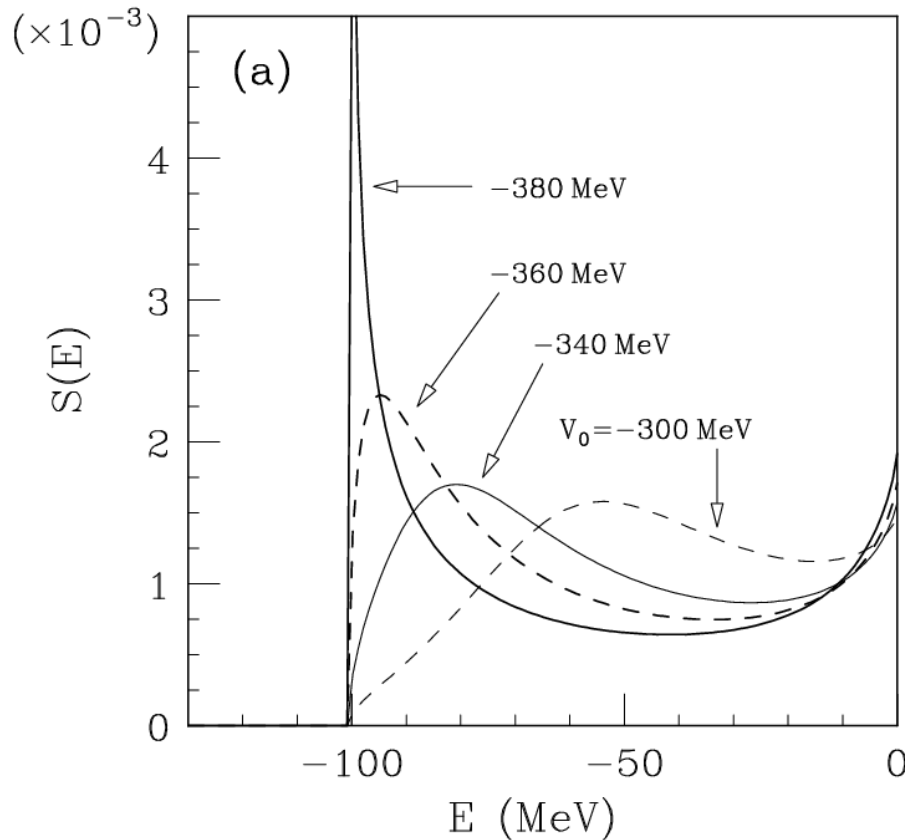
$$\begin{bmatrix} U_1(r) & U_{1,2}(r) \\ U_{2,1}(r) & U_2(r) \end{bmatrix} = \begin{bmatrix} V_1 + iW_1 & V_c \\ V_c & V_2 + iW_2 \end{bmatrix} \exp[-(r/b)^2]$$

2核子吸収過程は $U_1(r)$ の虚数部分 W_1 として記述する。

- 非相対論的扱い (single-channel 計算は相対論的)

◆ Comparison between single- and coupled-channel

Single-channel model

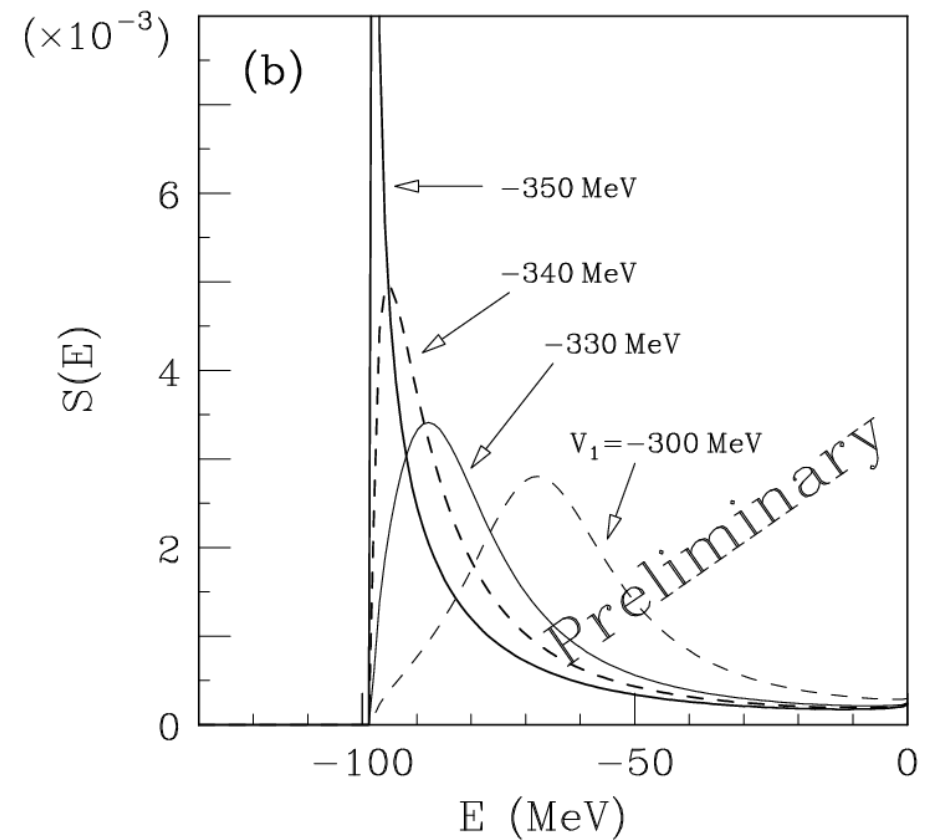


V_0 is changed.

$W_0 = -93$ MeV,

$B_1^{(\pi\Sigma N)} = 1.0$, $B_2^{(\pi\Sigma)} = 0.0$

Coupled-channel model



V_1 is changed.

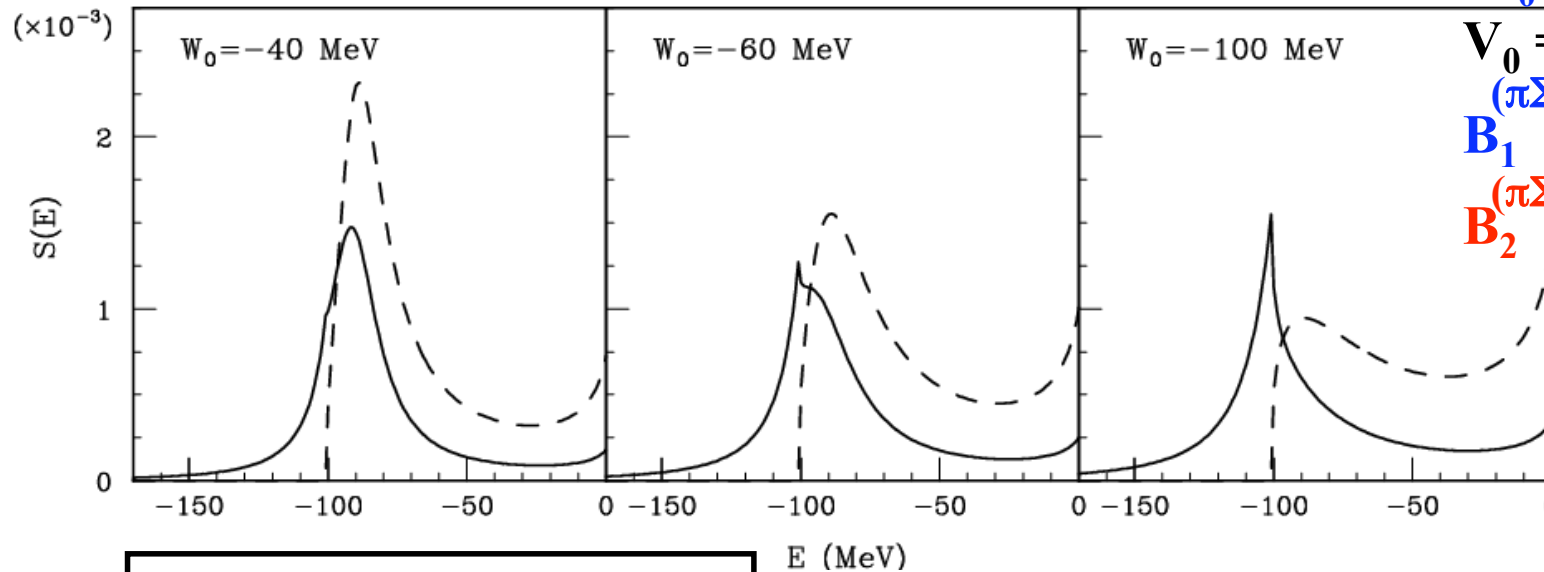
$V_C = +100$ MeV,

$V_2 = -120$ MeV,

$W_1 = 0$ MeV

◆ Comparison between single- and coupled-channel

Single-channel model



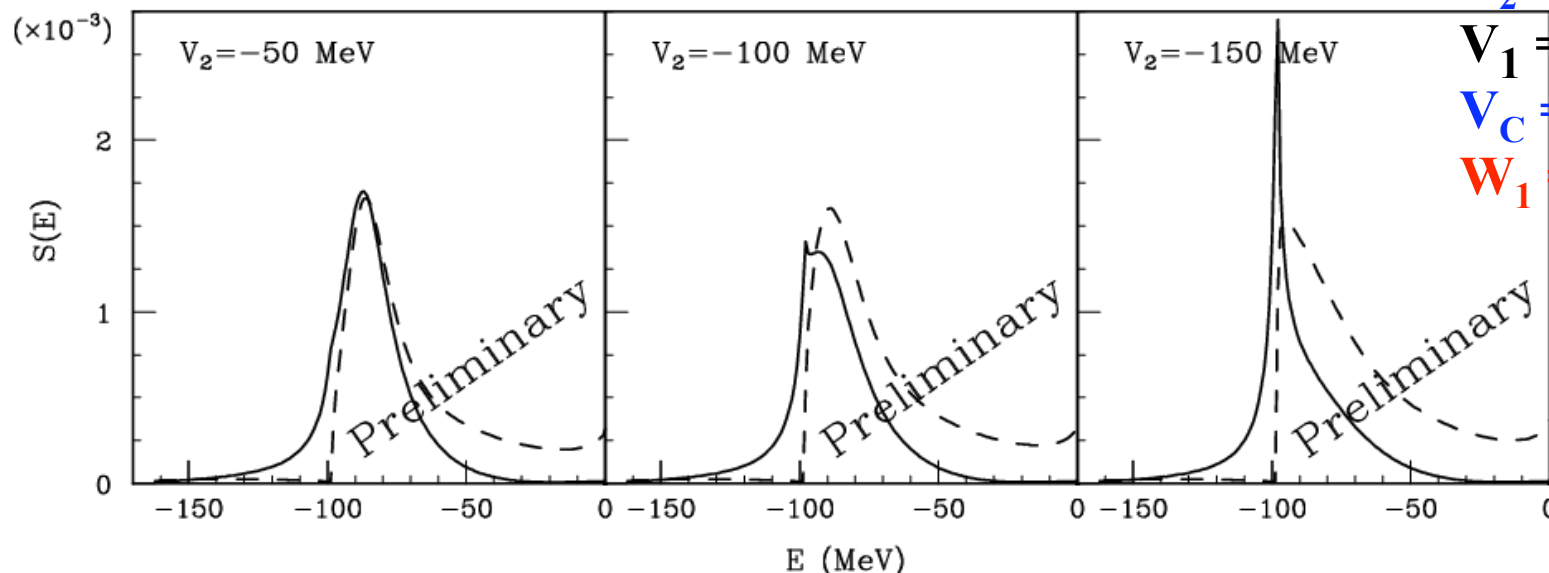
W_0 is changed.

$V_0 = -360$ MeV,

$B_1^{(\pi\Sigma N)} = 0.8,$

$B_2^{(\pi\Sigma)} = 0.2$

Coupled-channel model



V_2 is changed.

$V_1 = -360$ MeV,

$V_C = +100$ MeV,

$W_1 = -10$ MeV.

◆ Summary

- DHW & YA: 1核子 & 2核子吸収スペクトルの双方ピークが現れる。
- SGM: 2核子吸収スペクトルのみにカスプ構造が現れる。
- FINUDA: 2核子吸収スペクトルのみにピークが現れる。
⇒ 2核子吸収スペクトルにはいずれの場合も何らかの形でシグナルが観測されると期待できる。
- 単一チャンネル計算において、スペクトルの形は複素E平面上のポールの「動き」と関係づけて理解できる。
- Preliminaryな結合チャンネル計算は定性的には phase space factor を用いた単一チャンネル計算と一致する。
同じポールの位置を与えるポテンシャルで、スペクトルがどれだけ定量的に異なるかを調べるのが次の課題。